Surface Science 67 (1977) 180–194

ADSORPTION-DESORPTION PROPERTIES AND SURFACE STRUCTURAL CHEMISTRY OF CHLORINE ON Cu(111) AND Ag(111)

P.J. GODDARD and R.M. LAMBERT

Department of Physical Chemistry, University of Cambridge, Cambridge CB2 1EP, England

Received 14 February 1977; manuscript received in final form 13 May 1977

The adsorption, desorption, and structural properties of chlorine adlayers on Cu(111) and Ag(111) have been studied by LEED, Auger, $\Delta\varphi$, and thermal desorption measurements. Ancillary experiments were also carried out on cuprous chloride for purposes of comparison with the Cu(111)–Cl data. Chlorine adsorption is rapid on both metals and follows precursor kinetics, the absolute initial sticking probabilities being ~1.0 (Cu) and ~0.5 (Ag). $\Delta\varphi$ results suggest that significant depolarisation of the chemisorption bond occurs at high coverages, the maximum values being +1.2 eV (Cu) and +1.8 eV (Ag). On Cu(111), adsorption leads to the formation of a sequence of well-ordered phases; in order of increasing coverage, these are as follows: $(\sqrt{3} \times \sqrt{3})R30°$, $(12\sqrt{3} \times 12\sqrt{3})R30°$, $(4\sqrt{7} \times 4\sqrt{7})R19.2°$, and $(6\sqrt{3} \times 6\sqrt{3})R30°$. On Ag(111) $(\sqrt{3} \times \sqrt{3})R30°$, and (10×10) structures are observed. All six structures are susceptible to a straightforward interpretation in terms of coincidence lattices resulting from the progressive uniform compression of a hexagonal layer of Cl atoms. This interpretation is consistent with all the experimental results, and gives values for the nearest-neighbour Cl–Cl spacing on both Cu(111) and Ag(111) which are in good agreement with other work on other surfaces. Chlorine desorbs exclusively as atoms from both metals with first-order desorption kinetics, and apparent desorption energies of 236 (Cu) and 209 (Ag) kJ mol^{-1}. These values, which depend on an assumed pre-exponential factor of 10^{13} s^{-1}, are shown to be inconsistent with the thermochemical constraints on the system necessitated by the complete absence of Cl_2 desorption. Lower limits for the pre-exponential factors are then deduced, and the values are found to be consistent with the differences between the Cu–Cl and Ag–Cl systems.

1. Introduction

Previous studies of halogen adsorption on the Group IB metals have included the following systems: Cu(100)–Cl_2 [1], Ag(111) (100) (110)–Cl [2–4], Ag(111)–I_2 [5,6], Au(100)–Cl [7]. Broadly speaking, the structural results have been interpreted either in terms of simple chemisorption overlayers [1,4,6,7] or in terms of "surface corrosion" or reconstruction models involving rearrangement of surface metal atoms [2,3]. In the present paper we examine the adsorption of chlorine on Cu(111) and Ag(111). The Cu(111)–Cl_2 system has not been studied previously, and although Rovida and co-workers have investigated chlorine structures on Ag(111), they used ethylene dichloride rather than Cl_2 as the chlorinating agent

[2,3]. This point is of significance because, on the one hand, ethylene dichloride is the chlorinating agent used industrially to improve the selective oxidation of ethylene, whereas, on the other hand, the accepted mechanism for its effectiveness involves deposition of Cl adatoms on the Ag surface [9]. It is therefore of interest to compare our results, which unambiguously refer to the adsorption of chlorine alone, with those of Rovida et al.

2. Experimental

The ultra-high vacuum chamber, its contents, and mode of operation have been described elsewhere in considerable detail [10]. Base pressures of $\sim 2 \times 10^{-11}$ Torr were routinely available in this system, and the experimental geometry was such as to permit efficient line-of-sight collision-free sampling of desorbing reactive species by direct beaming between crystal front face and mass spectrometer ionizer. $\Delta\varphi$ measurements were carried out by the electron beam-retarding potential technique. The preparation and mounting [10] of the Ag(111) specimen have already been described. The Cu(111) specimen was cut from an ingot of 99.999% purity (Metals Research Ltd.) after orienting to within 0.25° of [111]. After mechanical polishing, the Cu(111) specimen was chemically polished for a few minutes in a mixture consisting of equal volumes of concentrated nitric, acetic, and orthophosphoric acids. This procedure reliably resulted in a surface with an excellent specular finish, and the Cu specimen was mounted in the same fashion as the Ag one. Preliminary Auger examination showed the Cu(111) specimen to be extensively contaminated with S, C, and Cl. These impurities were removed by Ar^+ bombardment (10^{-2} A m^{-2} at 300 eV for several hours), and subsequent annealing of the crystal at 1000 K for 2 min produced a sharp (1 × 1) LEED pattern. However, prolonged heating led to the degradation of this LEED pattern and the reappearance of the S Auger signal. This sulphur, presumably diffusing from the bulk, was eventually removed by repeated cycles of heating and Ar^+ bombardment over a period of 24 h.

We have already described the cleaning procedure for Ag[10] and figs. 1A, 1B show the LEED patterns from clean annealed Cu(111) and Ag(111) respectively. Subsequent exposure of these surfaces to laboratory atmosphere resulted in the accumulation of surface S which was readily removed by Ar^+ bombardment. In the case of Cu(111), the surface sulphide resulting from atmospheric exposure was remarkably well-ordered and stable. Fig. 1C shows the LEED pattern obtained from such a surface immediately after pumpdown and bakeout and *without* any other treatment. This pattern is identical with that which has already been reported for S adsorption on Cu(111) [11]. Surface Cl resulting from Cl_2 adsorption experiments could be removed completely by heating at 1020 K (Cu) or 920 K (Ag). An interesting feature of the early Cu/Cl_2 desorption experiments was ascribed to the presence of small amounts of Na in the Cu. This Na was observed to evaporate at $\geqslant$900 K, at which temperatures evaporation of the Cu lattice itself becomes appre-

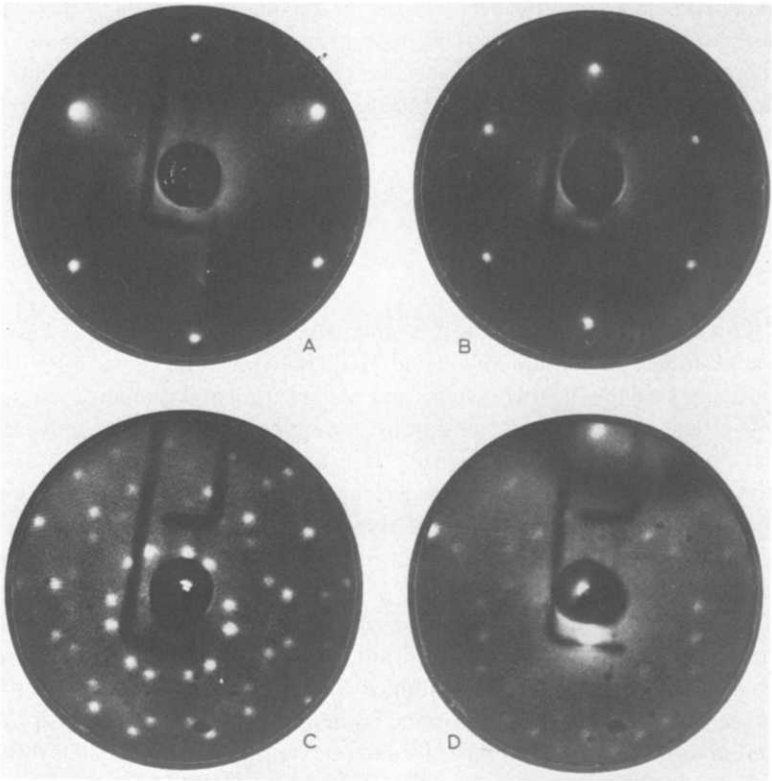

Fig. 1. LEED patterns: (A) Cu(111) clean surface, 111 V; (B) Ag(111) clean surface, 113 V; (C) Cu(111)–S, 90 V; (D) Cu(111)–Na + Cl, 64 V.

ciable, and it was removed only slowly by Ar^+ bombardment and heating. However, dosing the crystal with Cl_2 appeared to bring Na to the surface very efficiently, from whence it could be desorbed as NaCl at a much lower temperature (~660 K) than either sodium or chlorine themselves. This is readily understandable in terms of elementary thermodynamic considerations, given the large bond energy (409 kJ mol^{-1}) of the NaCl diatomic molecule [12]. Fig. 2C shows such NaCl desorption spectra recorded at 23 (Na^+), 35 (Cl^+), and 78 ($NaCl^+$) amu. Essentially identical spectra could be obtained by dosing the surface with Na from an aluminosilicate ion source, followed by exposure to Cl_2 (ordered surface structures were also formed under these conditions, e.g. fig. 1D). This supports the view that the original NaCl desorption resulted from the combination of adsorbed chlorine with impurity sodium, and suggests that Cl_2 may be a useful reagent for removing alkalis from metal crystals. The prolonged use of Cl_2 in the UHV system led to problems which are to be expected as a result of the corrosion of various compo-

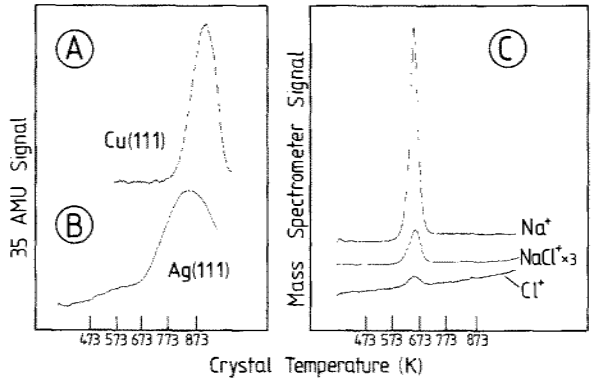

Fig. 2. Thermal desorption spectra: (A) from Cl saturated Cu(111); (B) from Cl saturated Ag(111); (C) from Cu(111)–Na + Cl. Heating rates 8 (Cu) and 15 (Ag) K s^{-1}.

nents, the most serious difficulty encountered being the periodic failure of precision leak valves.

3. Results

3.1. Cu(111)–Cl_2

Chlorine was found to adsorb on Cu(111) at 300 K with a very high sticking probability, the surface saturating after an exposure of ~1 L (1 L = 1 Langmuir = 10^{-6} Torr sec). Thermal desorption experiments showed that *Cl atoms were the only desorption product*, there being no detectable desorption of Cl_2 or copper chlorides. This Cl desorption occurred with apparent first-order kinetics, and fig. 2A shows a desorption spectrum from a surface saturated with Cl_2 at 300 K. Assuming a pre-exponential factor of 10^{13} s^{-1} leads to a value of ~236 kJ mol^{-1} for the desorption energy of atomic Cl from Cu(111). The desorption data provide a reliable measure of relative surface coverage, and may be used to construct the uptake curve for chlorine adsorption. These data are plotted in fig. 3; it can be seen that the system follows precursor state kinetics, the sticking probability remaining independent of coverage until the surface is virtually saturated. The crystal work function and Cl ($L_3M_{2,3}M_{2,3}$) Auger signal were also followed as a function of exposure at 300 K. These data are shown in fig. 3 along with the thermal desorption data, all three sets being normalised to the same ordinate scale. It can be seen that the $\Delta\varphi$ results saturate first; they also show the greatest departure from linearity over the entire coverage range. The Auger spectrum of the saturated surface, which corresponds to $\Delta\varphi = +1.2$ eV, is shown in fig. 4B; no electron impact effects were observed. Flashing the crystal to 920 K removed all the chlorine, as monitored

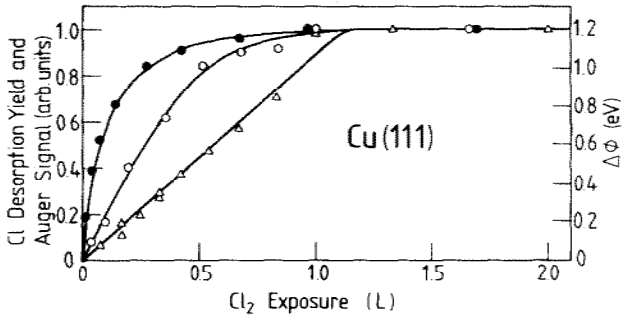

Fig. 3. Dependence of Cl desorption yield (□), Auger signal (○), and $\Delta\varphi$ (△), on Cl_2 exposure for Cu(111).

by Auger spectroscopy, and the work function returned to the clean surface value.

Chlorine dosing of the crystal at 300 K resulted initially in a marked increase in the background intensity of the LEED pattern. At $\theta/\theta_{max} \sim 0.65$ a $(\sqrt{3} \times \sqrt{3})R30°$ structure began to form, and this reached its maximum degree of perfection (as determined by photography and microdensitometry) at $\theta/\theta_{max} = 0.76 \pm 0.04$. This

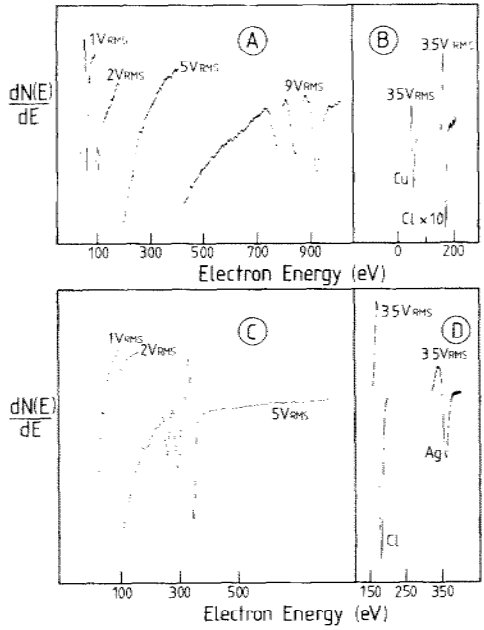

Fig. 4. Auger spectra at 2500 eV primary energy: (A) clean Cu(111); (B) from Cu(111)–Cl saturated surface; (C) clean Ag(111); (D) from Ag(111)–Cl saturated surface.

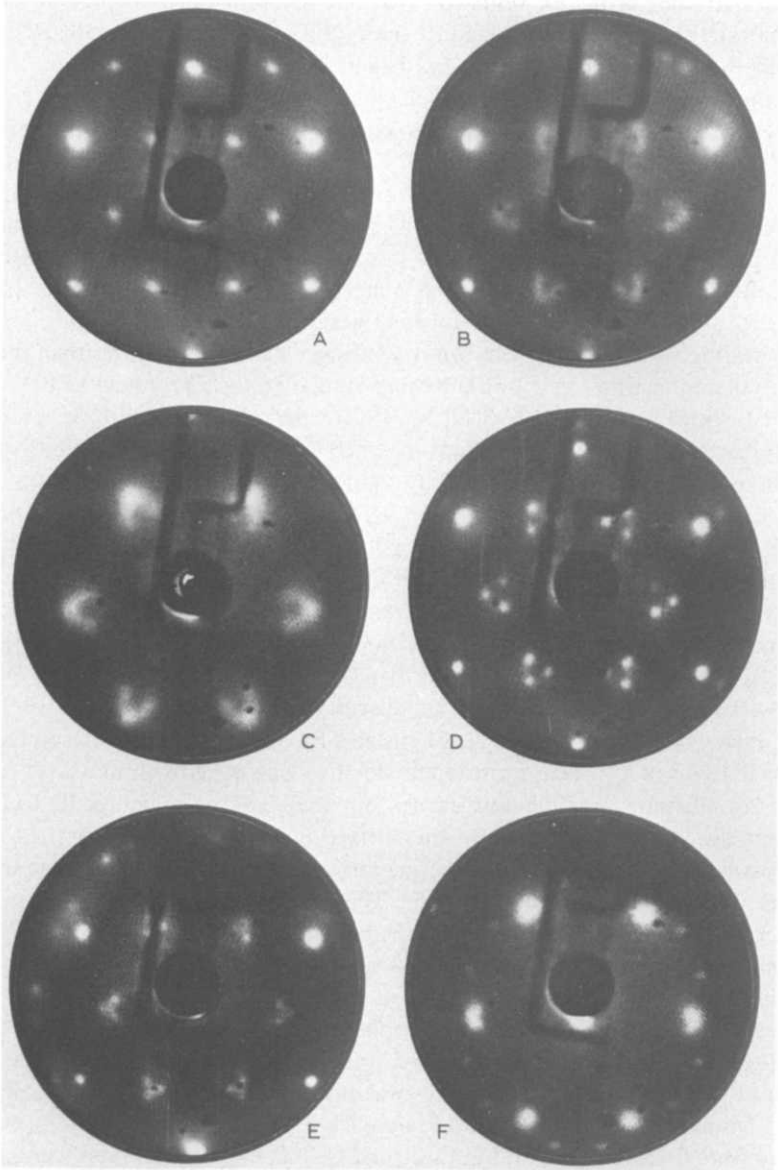

Fig. 5. LEED patterns: (A) Cu(111)–($\sqrt{3} \times \sqrt{3}$)R30°Cl, 120 V; (B) Cu(111)–Cl intermediate compression phase, 117 V; (c) same as B at 69 V; (D) Cu(111)–($6\sqrt{3} \times 6\sqrt{3}$)R30°Cl, 115 V; (E) Cu(111)–($12\sqrt{3} \times 12\sqrt{3}$)R30°Cl, 124 V; (F) Cu(111)–($4\sqrt{7} \times 4\sqrt{7}$)R19.2°Cl, 63 V.

LEED pattern (figure 5A) was very temperature-sensitive, being completely destroyed upon heating the crystal to only 350 K; cooling to 300 K restored the original pattern. Further exposure to Cl_2 at 300 K resulted in a broadening and partial splitting of the overlayer beams in the $(\sqrt{3} \times \sqrt{3})$ pattern (figs. 5B, 5C). It can be seen that each overlayer beam has begun to split into a triplet whose components move towards the positions which would be occupied by the overlayer beams from a (2×2) structure. This split-beam pattern is the saturation chlorine structure at 300 K. Heating this structure to 370 K, followed by cooling, greatly improved the long-range order, and the broad features of figs. 5B, 5C separated to form well-resolved triplets (fig. 5D). Further weak beams can also be observed in this final LEED pattern, and we will denote the structure to which it corresponds as $(6\sqrt{3} \times 6\sqrt{3})R30^\circ$-Cl. This structure showed much greater thermal stability than the $\sqrt{3}$ structure, and could be observed for long periods at temperatures up to ~620 K. Upon heating to 370 K a surface whose coverage was somewhat less than the saturation value (and showing a LEED pattern similar to fig. 5B), a new LEED pattern (fig. 5E) showing weak $(12\sqrt{3} \times 12\sqrt{3})R30^\circ$ periodicities could be produced. Finally, heating the saturated surface to ~720 K (at which temperature Cl desorption becomes appreciable) followed by cooling, led to the formation of a fourth ordered phase which indexes as a $(4\sqrt{7} \times 4\sqrt{7})R19.2^\circ$ structure (fig. 5F). Broadened beams from coexisting domains of the $\sqrt{3}$ structure are also visible in figure 5F. A weak $4\sqrt{7}$ pattern could also be obtained by careful Cl_2 dosing of a well-formed $\sqrt{3}$ structure at 300 K. We can therefore arrange these structures in order of increasing chlorine surface concentration as follows: $(\sqrt{3} \times \sqrt{3})R30^\circ < (4\sqrt{7} \times 4\sqrt{7})R19.2^\circ < (12\sqrt{3} \times 12\sqrt{3})R30^\circ < (6\sqrt{3} \times 6\sqrt{3})R30^\circ$. Proposed structures for three of these phases are shown in figs. 9A, 9B, 10 and discussed in section 4.

In their work on the Ag(111)–Cl system, Rovida et al. [2,3] interpreted their results in terms of a surface corrosion model involving the growth of a layer of AgCl on an Ag substrate. We therefore carried out some control experiments to investigate the species evaporating from the surface of a sample of anhydrous CuCl, in order to assess whether or not the thermal properties bore any resemblance to those of the Cu(111)–Cl adsorption system. These experiments were carried out in a small auxiliary UHV system in which the line-of-sight sampling between mass spectrometer ionizer and CuCl specimen was very similar to that in the main apparatus. The specimen consisted of a small bead of CuCl which was melted on to a 0.35 mm diameter Ta wire to which a thermocouple was attached. After thoroughly outgassing the CuCl at 500 K (which removed principally H_2O), the temperature dependence of the various desorbing species was investigated. The only species observed in the temperature range 300–600 K were Cl, Cl_2, Cu, CuCl, and Cu_2Cl_2. No ionic species were detected. The Cl, Cu, CuCl, and Cu_2Cl_2 evaporation rates were not sufficiently reproducible to permit accurate equilibrium measurements, but such measurements were possible in the case of Cl_2. Fig. 6 shows a plot of ln (70 amu signal) against $1/T$. It can be seen that there are two temperature regimes which are characterised by different apparent activation energies for Cl_2 desorption, the relevant values being ~168 and ~93 kJ mol^{-1}.

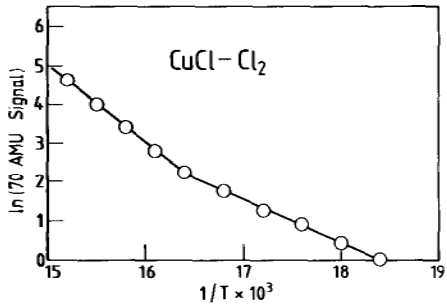

Fig. 6. Evaporation of Cl_2 from crystalline CuCl.

3.2. Ag(111)–Cl

Chlorine adsorption on Ag(111) was also found to be rapid at 300 K, and just as with Cu(111), desorption was found to occur exclusively as atomic Cl. Fig. 2B shows the desorption spectrum of a chlorine saturated surface from which one may derive a desorption energy of ~209 kJ mol^{-1}, assuming 10^{13} s^{-1} as the pre-exponential factor. The desorption spectra were significantly broader than with Cu(111), and appeared to indicate first-order desorption kinetics, but were not particularly well-suited to the measurement of relative coverage. This is because the desorption sweep had to be stopped at ~950 K – the temperature at which Ag evaporation becomes important [10] – at which point Cl evaporation was incomplete. There also appeared to be an appreciable contribution to the desorption spectrum from the crystal supports at these higher temperatures. Fig. 7 shows the dependence of $\Delta\varphi$ and the chlorine Auger signal on Cl_2 exposure, while fig. 4D shows the Auger signal from the Cl saturated surface. Once again it can be seen that the $\Delta\varphi$ data saturate before the Auger data, with $\Delta\varphi_{max}$ = +1.8 eV. This is considerably higher than the value of +0.9 eV which was obtained by Rovida et al. [2,3]. The relative intensity of the saturation chlorine Auger signal obtained by these authors was also much smaller than in the present work. It should be recalled that

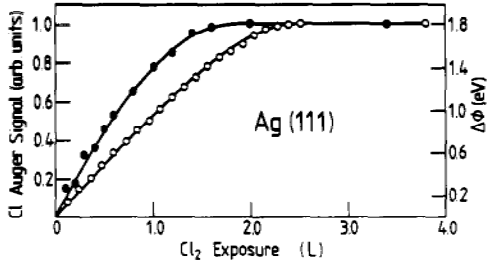

Fig. 7. Dependence of Cl Auger Signal (○) and $\Delta\varphi$ (△) on Cl_2 exposure for Ag(111).

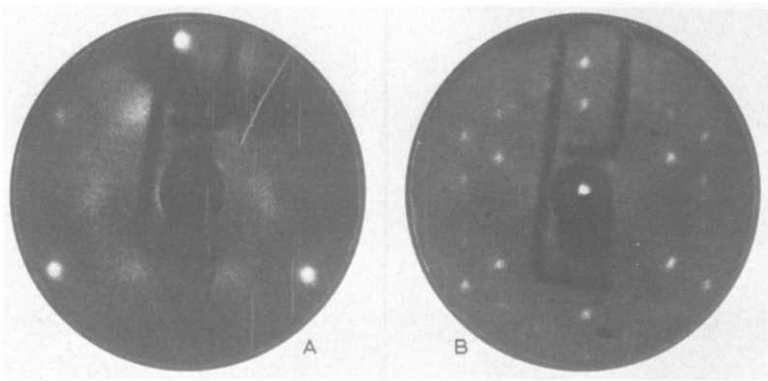

Fig. 8. LEED patterns: (A) Ag(111)–($\sqrt{3} \times \sqrt{3}$)R30°Cl, 85 V; (B) Ag(111)–(10 × 10)Cl, 86 V.

Rovida et al. [2,3] used high temperature, high pressure treatment with ethylene dichloride as the means of chlorinating their surfaces.

LEED observations showed that at low to intermediate coverages (~1.0–1.8 L Cl_2 at 300 K) an extremely poorly ordered ($\sqrt{3} \times \sqrt{3}$)R30° structure was formed. This structure could not be improved by thermal treatment, and a typical LEED pattern is shown in fig. 8A. Rovida et al. [2] also reported the formation of a poorly ordered $\sqrt{3}$ structure in their ethylene dichloride experiments, but did not show any LEED patterns. With increasing coverage at 300 K, the $\sqrt{3}$ pattern of fig. 8A was replaced by a new pattern which reached its maximum degree of perfection at saturation coverage, without any thermal treatment. This pattern (fig. 8B) showed both sharp diffraction beams and a high background intensity. Rovida et al. [2] observed a similar pattern which they ascribed to a "distorted 3 × 3" structure. We associate the pattern in figure 8B with a (10 × 10) structure which is shown in fig. 11 and discussed in section 4. The (10 × 10) structure disordered irreversibly on heating to ~650 K. If we use the $6\sqrt{3}$ and (10 × 10) structures as a guide to the saturation coverage on the Cu and Ag surfaces respectively (see sections 4.1, 4.2), then the data of figs. 3 and 7 may be used to obtain the absolute values of the intial sticking probability (S_0) of Cl_2 on the two surfaces. The results are S_0(Cu(111)) ~ 1.0, and S_0(Ag(111)) ~ 0.5, assuming that each Cl_2 adsorbs dissociatively to give two Cl adatoms. Both values are uncertain to within ±50%, even after allowing for gauge sensitivity to Cl_2 (13), due to uncertainty in the mass-spectrometric measurement of Cl_2 partial pressure during exposure to chlorine.

4. Discussion

Rovida et al. [2] have interpreted their "distorted 3 × 3" structure in terms of the growth of a monolayer of AgCl on Ag(111), and have also used this approach to

account for the Ag(100)–c(2 × 2)Cl structure. On the other hand, we have chosen to interpret *all* the structures reported in the present work in terms of simple chemisorption overlayers, and so this calls for some explanation. Zanazzi, Jona et al. [4] have recently carried out a detailed LEED intensity analysis of the Ag(100)–c(2 × 2)Cl structure, and it was shown to correspond to simple Cl atom chemisorption in fourfold sites. Further evidence against reconstruction in Ag–halogen systems is provided by the work of Forstmann [6] whose analysis of the Ag(111)–($\sqrt{3} \times \sqrt{3}$)I LEED data [5] showed this to be a chemisorption overlayer structure. Equally, in the case of Cu, Delamare [1] has inferred from the Debye–Waller factor of the Cu(100)–c(2 × 2)Cl structure that the metal surface does not undergo reconstruction. These indications, taken together with the results of the present work in relation to the $\Delta\varphi$ and Auger curves for both Ag and Cu (no discontinuities) and the desorption data (only one first-order Cl peak at all coverages), suggest that we are dealing with simple chlorine atom chemisorption at all coverages up to and including saturation coverage. We therefore take the view that Cl_2 chemisorbs dissociatively on both Cu(111) and Ag(111), that reorganisation of the metal surface does not occur, and that all four Cu–Cl structures and both Ag–Cl structures are to be interpreted in these terms. Some additional support for this view comes from the experiments with CuCl. It seems clear that the thermal properties of CuCl bear little, if any, resemblance to those of Cu(111)–Cl. Thus Cu, CuCl, Cu_2Cl_2, and Cl_2 are observed as major evaporation products along with Cl, and although the larger of the two measured enthalpies for chlorine loss is of the order of the chlorine desorption energy from Cu(111), it refers to the evaporation of molecules and *not* atoms. (It is possible that the values of ~93 and ~168 kJ mol^{-1} for Cl_2 evaporation correspond to situations in which the rate limiting steps are a surface process and bulk diffusion respectively [14].) All six of the LEED patterns reported above are capable of a natural and straightforward interpretation in terms of coincidence lattices between the (111) mesh and a hexagonal layer of Cl atoms. The observed structures evolve as the chlorine layer, retaining its sixfold symmetry, compresses uniformly with increasing coverage. Knowledge of the order of evolution with coverage (and in the case of the $6\sqrt{3}$ and $\sqrt{3}$ structures on Cu(111) the *actual relative coverage* is known rather accurately) permits an essentially unambiguous assignment of the structures.

4.1. Cu(111)–Cl structures

Experiment shows that $\theta_{Cl}(6\sqrt{3}) : \theta_{Cl}(\sqrt{3}) = 1 : 0.76 \pm 0.04$. Let us begin with the $\sqrt{3}$ structure and assume that it corresponds to a coincidence lattice with $\theta_{Cl} = 1/3$ (coverages measured relative to number density of Cu atoms in (111) plane) as opposed to $\theta_{Cl} = 2/3$. Let the Cu–Cu periodicity along $[2\bar{1}\bar{1}]$ be α, then this requires that there be one Cl atom per length α along $[2\bar{1}\bar{1}]$, and the corresponding structure is shown in figure 9A. Thus to produce the more concentrated $6\sqrt{3}$ structure from the $\sqrt{3}$ structure requires us to pack more than six Cl atoms

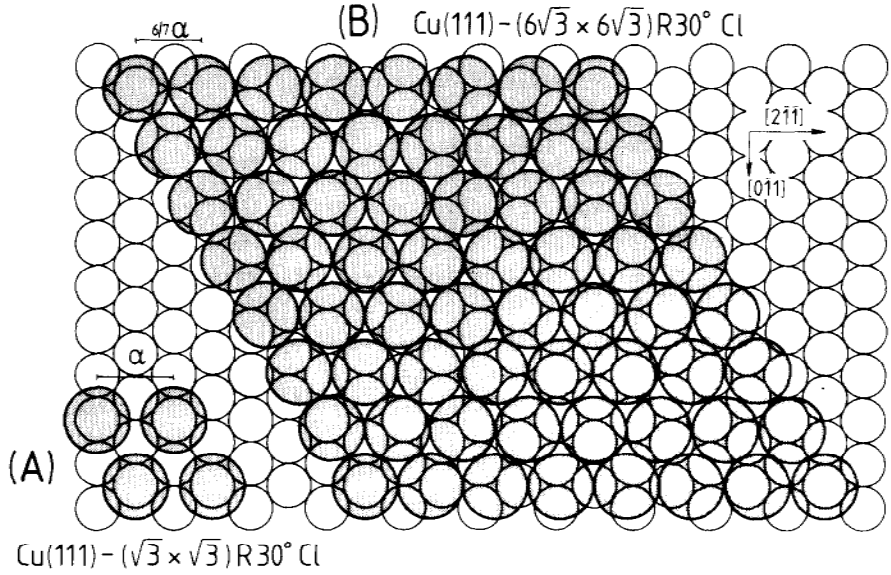

Fig. 9. Proposed surface structures: (A) Cu(111)–($\sqrt{3} \times \sqrt{3}$)R30°Cl; (B) Cu(111)–($6\sqrt{3} \times 6\sqrt{3}$)R30°Cl. Open circles = Cu, shaded circles = Cl.

into the distance $6a$ along [2$\bar{1}\bar{1}$]. This number must be 7, 11, or any higher number; 8, 9, 10, are not permitted because they would lead to other coincidence structures. Eleven seems like the largest physically reasonable number, but would correspond to $\theta_{Cl} = 1.12$ and a Cl–Cl spacing of 2.46 Å, which is exactly equal to the Cl muffin-tin diameter deduced by Zanazzi et al. [4] for Cl adsorbed on Ag(100). It is therefore highly unlikely and we rule it out. Furthermore, it leads to $\theta_{Cl}(6\sqrt{3}) : \theta_{Cl}(\sqrt{3}) = 1 : 0.298$ in disagreement with experiment. If we try $\theta_{Cl}(\sqrt{3}) = 2/3$ (instead of 1/3) then the 11 atom coincidence leads to $\theta_{Cl}(6\sqrt{3}) : \theta_{Cl}(\sqrt{3}) = 1.0595$ also in disagreement with experiment. On the other hand, taking $\theta_{Cl}(\sqrt{3}) = 1/3$ and assuming a seven Cl atom coincidence along [2$\bar{1}\bar{1}$] leads to $\theta_{Cl}(6\sqrt{3}) : \theta_{Cl}(\sqrt{3}) = 1 : 0.735$, in very good agreement with experiment. In addition to this, one deduces a Cl–Cl nearest-neighbour spacing of 3.86 Å for the $6\sqrt{3}$ saturated surface structure, which is rather close to the corresponding value of 3.64 Å deduced for the Cu(100)–c(2 × 2)Cl structure. We therefore assign the structures of the $\sqrt{3}$ and $6\sqrt{3}$ phases as shown in figs. 9A, 9B. It is worth noting that the very considerable temperature sensitivity of the $\sqrt{3}$ LEED pattern and the good thermal stability of the $6\sqrt{3}$ pattern are consistent with the expected resistance to thermal disorder of the two proposed structures. Having fixed on the structures of the most concentrated and most dilute ordered phases, those of the intermediate $4\sqrt{7}$ and $12\sqrt{3}$ phases follow naturally. The $12\sqrt{3}$ is derived from $6\sqrt{3}$ by a small uniform expansion of the Cl lattice to give a thirteen Cl atom coincidence in a length 12α along

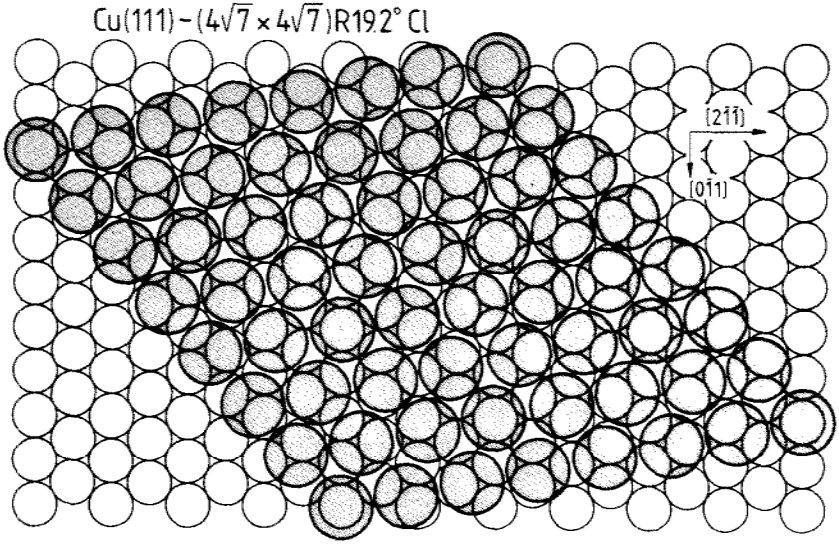

Fig. 10. Proposed structure for Cu(111)–(4$\sqrt{7}$ × 4$\sqrt{7}$)R19.2°Cl. Open circles = Cu, shaded circles = Cl.

[2$\bar{1}\bar{1}$]. It is *very* similar to the 6$\sqrt{3}$ phase, and we do not reproduce it here. The 4$\sqrt{7}$ structure is derived from the $\sqrt{3}$ by a small uniform compression and rotation of the Cl layer, and is shown in fig. 10. The structural and coverage data are summarised in table 1.

4.2. Ag(111)–Cl

In the case of Ag we conclude that, as with Cu, the $\sqrt{3}$ phase which appears initially corresponds to a chemisorbed layer with $\theta_{Cl} = 1/3$. Its structure is therefore the same as that illustrated in figure 9A, except for a change of scale. It is of interest to consider why the Ag$\sqrt{3}$ structure is so very poorly ordered compared

Table 1

Chlorine structure	θ_{Cl}	r_{Cl-Cl}(Å)
Cu($\sqrt{3}$ × $\sqrt{3}$)R30°	1/3	4.50
Cu(12$\sqrt{3}$ × 12$\sqrt{3}$)R30°	0.39	4.09
Cu(4$\sqrt{7}$ × 4$\sqrt{7}$)R19.2°	0.44	3.93
Cu(6$\sqrt{3}$ × 6$\sqrt{3}$)R30°	0.45	3.86
Ag($\sqrt{3}$ × $\sqrt{3}$)R30°	1/3	5.00
Ag(10 × 10)	0.49	4.12

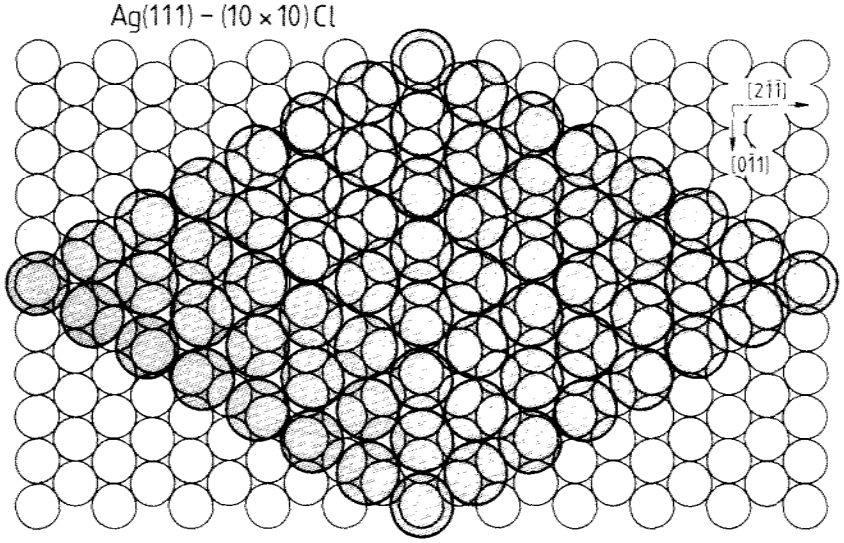

Fig. 11. Proposed structure for Ag(111)–(10 × 10)Cl. Open circles = Ag, shaded circles = Cl.

with the well-ordered Cu$\sqrt{3}$ structure. One plausible suggestion might be that this effect is associated with the ~12% expansion of the (111) surface mesh in going from Cu to Ag which could permit greater disorder in the already dilute chlorine layer. Proceeding as before, we conclude that the well-ordered (10 × 10) structure which characterises the saturated surface is derived from the $\sqrt{3}$ phase by uniform compression and rotation of the hexagonal Cl layer. The proposed structure is shown in fig. 11, and corresponds to a Cl–Cl nearest-neighbour spacing of 4.12 Å, which is to be compared with the value of 4.20 Å deduced for the Ag(100)–c(2 × 2)Cl case [4]. It seems clear that there are close similarities between the chlorine structures observed in this work and those reported [2] by Rovida et al. in their work with Ag(111)–ethylene dichloride. This is consistent with the suggestion that the role of ethylene dichloride in the catalytic epoxidation of ethylene is that of depositing Cl adatoms on the Ag surface. However, the lower values of $\Delta\varphi_{max}$ and Cl saturation Auger signal which were reported by these authors suggest that the Cl coverages which they achieved were smaller than in the present work.

It is somewhat interesting to note that in *all* the well-resolved long-periodicity structures which were observed in this work (4$\sqrt{7}$, 12$\sqrt{3}$, 6$\sqrt{3}$, and (10 × 10), the most intense extra feature beams were always those corresponding to the Cl–Cl periodicity of the overlayer. In no case are all the predicted coincidence-net beams observed. This, of course, is a common observation for such long-periodicity coincidence lattices (e.g. Au(100)-(5 × 20), Pt(100)-(5 × 20).

4.3. $\Delta\varphi$ and thermal properties

With both metals the $\Delta\varphi$ versus Cl_2 exposure curve saturates before the Cl Auger and (for Cu) thermal desorption yields. This suggests that significant depolarisation of the metal–Cl bond occurs at high coverages for both Cu and Ag. The fact that chlorine desorption occurs exclusively as atomic Cl from both metals at all coverages deserves some comment. Since this desorption pathway is preferred over the desorption of molecular Cl_2, one may reasonably conclude that the activation energy to atomic desorption is lower than that for molecular desorption. This is simply the result of the relatively low Cl_2 bond energy (cf. the associative desorption of CO and N_2 from metal surfaces). Thus for the reactions

$$Cl(a) \rightarrow Cl(g)\,, \tag{1}$$

$$2Cl(a) \rightarrow Cl_2(g)\,. \tag{2}$$

(2) is less favourable than (1) because breaking the second metal–Cl bond is not compensated for by making the Cl–Cl bond. Given that Cl_2 adsorption is non-activated, so that the activation energy to desorption may be equated to the desorption enthalpy, we can write the bond energy inequality

$$D_{M-Cl} < 2D_{M-Cl} - D_{Cl-Cl}\,,$$

whence

$$D_{Cl-Cl} < D_{M-Cl}\,.$$

Now $D_{Cl-Cl} = 243$ kJ mol^{-1} [15], whereas the estimated values for D_{M-Cl} from this work are 236 (Cu) and 209 (Ag) kJ mol^{-1}. Clearly both these D_{M-Cl} values are somewhat at variance with experiment which demands that they should be greater than 243 kJ mol^{-1}. The answer resides in the fact that these values were calculated from desorption spectra by using an arbitrarily chosen pre-exponential factor (υ) of 10^{13} s^{-1}. It is instructive to calculate the values of υ which would make the experimentally derived D_{M-Cl} values $\geqslant D_{Cl-Cl}$, hence fulfilling the conditions for Cl atom desorption to become possible. The result is $\upsilon(Cu) \geqslant 2.7 \times 10^{13}$ s^{-1}, and $\upsilon(Ag) \geqslant 1.5 \times 10^{15}$ s^{-1}. Thus very little change in the assumed value of υ is required to bring the Cu results into line with observation, but a significant increase is called for in the case of Ag. This suggests that the transition state to chlorine desorption from Cu(111) does have just one vibrational degree of freedom, whereas on Ag(111) additional degrees of freedom are available – possibly a strongly-hindered translation or low frequency oscillation between different surface sites. This could also be the result of the greater lattice spacing on Ag(111) as compared with Cu(111).

Acknowledgement

We are grateful to I.C.I. Ltd. for financial support, and to Dr. T. Edmonds for helpful discussions.

References

[1] F. Delamare, Compt. Rend. (Paris) 275C (1972) 753.
[2] G. Rovida, F. Pratesi, M. Maglietta and E. Ferroni, Japan. J. Appl. Phys. Suppl. 2, Part 2 (1974) 117.
[3] G. Rovida and F. Pratesi, Surface Sci. 51 (1975) 270.
[4] E. Zanazzi, F. Jona, D.W. Jepsen and P.M. Marcus, Phys. Rev. B14 (1976) 432.
[5] W. Bernt, Japan. J. Appl. Phys. Suppl. 2, Part 2 (1974) 653.
[6] F. Forstmann, Japan. J. Appl. Phys. Suppl. 2, Part 2 (1974) 657.
[7] D.G. Fedak, J.V. Florio and W.D. Robertson, in: The Structure and Properties of Solid Surfaces, Ed. G.A. Somorjai (Wiley, New York, 1969) p. 74-1.
[8] R.G. Meisenheimer and J.N. Wilson, J. Catalysis 1 (1962) 151.
[9] P.A. Kilty, N.C. Rol and W.M.H. Sachtler, in: Catalysis, Ed. J.W. Hightower (North-Holland, Amsterdam, 1973) p. 929.
[10] R.A. Marbrow and R.M. Lambert, Surface Sci. 61 (1977) 317, 329.
[11] J.L. Domange and J. Oudar, Surface Sci. 11 (1968) 124.
[12] V.N. Kondrat' ev, Chemical Kinetics of Gas Reactions (Pergamon, 1964) p. 88.
[13] M.L. Shaw, Rev. Sci. Instr. 37 (1966) 113.
[14] G.M. Rosenblatt, in: Treatise on Solid State Chemistry, Vol. 6A (Surfaces 1), Ed. N.B. Hannay (Plenum, New York, 1976). ch. 1.
[15] A.G. Gaydon, Dissociation Energies and Spectra of Diatomic Molecules, 3rd ed. (Chapman and Hall, London, 1968) p. 268.